

Rock magnetism and magnetic anisotropy in folded sills and basaltic flows: A case study of volcanics from the Taimyr Peninsula, Northern Russia

ZHANG ShuWei^{1,2,3†}, J. Harald WALDERHAUG² & YANG YueJun⁴

¹ College of Computer Engineering and Software, Taiyuan University of Technology, Taiyuan 030024, China;

² Department of Earth Sciences, University of Bergen, Allègaten 41, 5007 Bergen, Norway;

³ State Key Laboratory of Geological Processes and Mineral Resources, China University of Geosciences, Beijing 100083, China;

⁴ Department of Applied Physics, Taiyuan University of Technology, Taiyuan 030024, China

Magnetic measurements were performed on apparently deformed igneous rocks of 23 sites from the southeastern part of the Taimyr Peninsula. Rock magnetism and reflected light microscopy analyses reveal that fine-grained titanomagnetites up to pure magnetites mainly carry the majority of magnetic fabrics in the sills, and that the slightly coarser Ti-poor or -medium titanomagnetites carry most magnetic fabrics in the basaltic flows. Magnetic anisotropies were determined by applying anisotropy of low-field magnetic susceptibility (AMS) on 180 unheated samples and 128 samples that had been previously heated to 600°C during a paleomagnetic study to detect heating effects on the anisotropy of magnetic susceptibility (AMS) properties of volcanic rocks. Laboratory heating significantly affects anisotropy variations of these igneous rocks corresponding to the mineralogical changes during the heat treatment.

sill, basalt, magnetic fabric, rock magnetism, Taimyr

The Taimyr Peninsula lies on the northern edge of the Eurasian landmass, between the Laptev and Kara seas, occupies a central position in the geologic setting of Arctic Siberia, and contains igneous, metamorphic and sedimentary rocks of Proterozoic-Cretaceous ages (Figure 1). Researches on Taimyr igneous rocks contribute to multidisciplinary investigations and understanding the tectonic evolution of a much wider area of Arctic Eurasia. Rock magnetic studies of the South Taimyr igneous complex (75°N, 100°E) (Figure 1) can not only better define magnetic carriers and their relative contribution to both the mean magnetic susceptibility and its anisotropy, but also provide a proof of elucidating timing and stability of the stable remanence. Based on the rock magnetic analysis, we reveal magnetic properties relating to initial grain-size variations, differential secondary chemical alterations of titanomagnetite (TM) phases, and original cooling rate differences^[1–4]. Laboratory

heating experiments are performed on Taimyr igneous rocks in order to get better defined AMS fabrics^[2,3,5]. A discussion was made by comparing the post-heating fabrics with the initial magnetic fabrics before heating. Heating produces AMS changes, which does not always correspond to simple enhancement of the magnetic fabric for all samples. One of the aims of the present work is to better understand magnetic properties and fabric changes after the heating.

1 Geological setting and sampling

The Taimyr Peninsula is traditionally divided into three units: North, Central and South Taimyr (Figure 1(b)).

Received August 14, 2007; accepted November 22, 2007

doi: 10.1007/s11434-008-0069-z

†Corresponding author (email: zhang.shuwei@163.com)

Supported by the Norwegian Research Council as a grant to HJW, Norwegian State Education Loan Fund (Register No. 1921471), SWEDARP and EUROPROBE

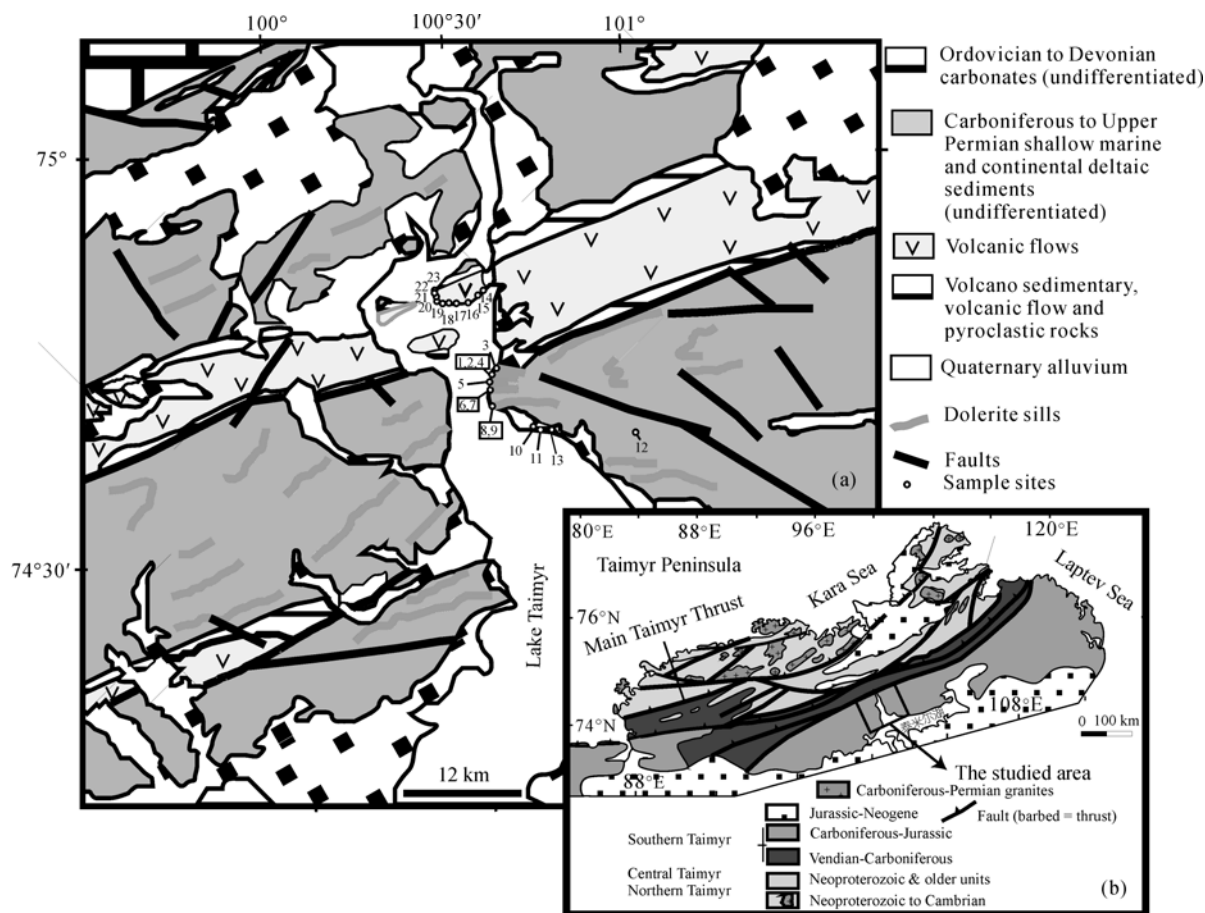


Figure 1 (a) Geological map (after Bezzubtsev et al.^[6]) of the studied area and location of the sampling sites (site numbers labeled 1, 2, etc.). (b) Location map of the Taimyr Peninsula within Arctic Siberia. Modified from Torsvik & Andersen^[2]. The study region is identified on the northern margin of Taimyr Lake.

Taimyr igneous rocks intrude and fold together with the Carboniferous-Lower Triassic continental classic succession around an ENE-WSW-trending axis, and their age is constrained by the fact that they are unconformably overlain by Early Jurassic sedimentary units (Figure 1). No Lower Triassic clastic sediments are present in the immediate studied area, although the Upper Permian through Lower Triassic clastic rocks have been reported elsewhere in South Taimyr^[8,9]. Attitudes of the sills dominantly vary between 84° – 119° with shallow dips lower than 28° , and are three to five-meter thick; the basaltic flows mainly strike between 59° – 80° with slightly steeper dips from 23° to 36° , and are three to five-meter thick with well-preserved columnar jointing. Their emplacement may be controlled by the NNW-SSE-trending folding event, E-W-trending thrusts and E-W strike-slip faults that have been recognized in the Taimyr. Collision of North Taimyr with South-Central Taimyr (North Siberia) generated the NNW-SSE com-

pression and could account for the three structural systems^[6,10]. The eruptive and intrusive rocks are generally given Permo-Triassic age designations^[6]. Paleomagnetic data give ages between 230 – 220 Ma^[11] and 250 – 220 Ma^[11] for the sills and basalts, respectively.

A total of 308 samples were prepared out of cylindrical cores drilled at 23 sites with a mixture of field coring and hand sampling. Both solar compass whenever possible and magnetic compass were used to orient all cores, and the solar compass can avoid magnetic confusion caused by the remanent magnetization of the sampled rocks.

2 Magnetic mineralogy

It is very important to determine the magnetic minerals in a rock since the AMS is caused by minerals with very different magnetic behavior. In the present study, the magnetic mineral property was identified using combined analysis of bulk magnetic properties, hysteresis

curves, reflected light microscopy and thermomagnetic curves. These techniques allow to characterize the ferromagnetic phases (magnetite and haematite), grain sizes and their relative contribution to the whole susceptibility in the rocks.

2.1 Thermomagnetic analysis and reflected light microscopy

Thermomagnetic analysis, the measurement of magnetization as a function of temperature, was used to identify magnetic minerals on a total of 34 specimens by measurement of their Curie temperatures (T_c), on a horizontal translation balance with a heating/cooling cycle of ca. 90 minutes in a field of 0.7 Tesla. The thermomagnetic curves are generally reversible and show a single T_c close to 580°C, suggesting a titanomagnetite approaching pure magnetite as the main magnetic min-

eral in the sills (S8 in Figure 2). The basalt flows show more variation and irreversible curves with T_c ranging from 435°C (S14) to 580°C (S17) (Figure 2), indicating a significant titanium content in the magnetic phase^[11,12].

Identification of opaque minerals may assist in determining the origin of magnetization and the degree of deuteric and low-temperature oxidation affecting the opaque phases, based on observations of polished sections and oil immersion. Figure 3 shows some typical mineral textures, with an oil immersion objective and high-resolution digital camera. TM is the main magnetic phase. In general, the sills display plenty of relatively large grains ranging from TM to crystals showing ilmenite lamellae (Figure 3(a), (b), (c)), sandwich type texture (as the dark brown lamellae through a polarizing microscope), attesting to a relatively slow initial cooling; Figure 3(a) illustrates a large TM crystal, partly altered

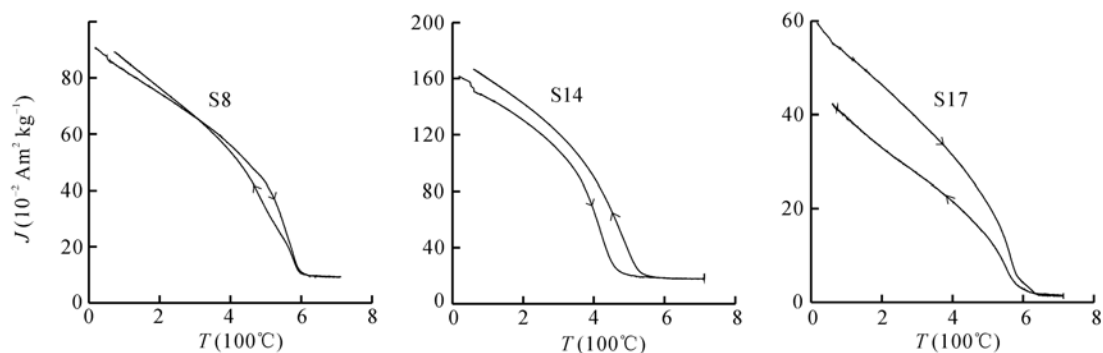


Figure 2 Representative thermomagnetic curves for the sills (site S8) and basaltic flows (site S14 and S17). The arrows indicate the direction of heating and cooling, respectively.

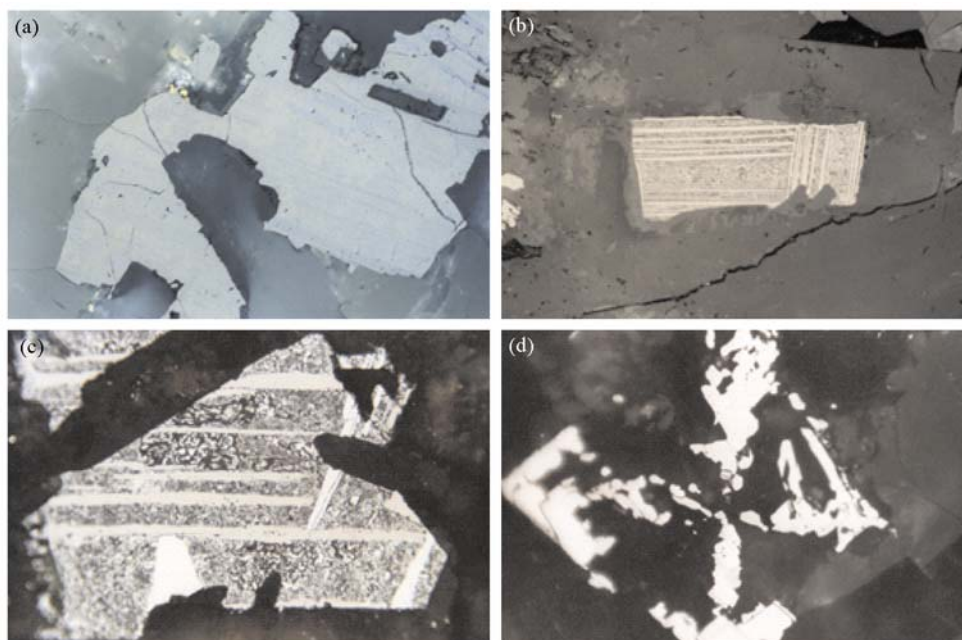


Figure 3 Representative microphotographs of oxide magnetic minerals showing typical mineral textures; the sills (a), (b) and (c); the basaltic flows (d).

to titanomaghemite along fractures; ilmenite may be either primary or may have resulted from oxy-exsolution (Figure 3(b)); titanohematite is homogeneously disseminated in the rock fragments presenting in fine grains and granular shapes (Figure 3(b), (c)); some shrinkage cracks and granular surfaces indicate low-temperature alteration (Figure 3(a), (b), (c)) leading to smaller magnetic “grains” due to fine subdivision of magnetic grains. In contrast, the basaltic flows illustrate homogeneous fine skeletal crystalline lattice^[11,12] (Figure 3(d)), consistent with a rapid cooling rate with little or no secondary alteration; occasionally, large TM grains are observed. Non-magnetic pyrite is present.

2.2 Bulk magnetic and hysteresis properties

Site mean values of intensities (J) and mean magnetic susceptibilities (Figure 5(a), (b)) for the sills are generally in 0.13–1.33 A/m and 3.19×10^{-3} – 1.44×10^{-2} SI (Table 2), respectively, and the basaltic flows illustrate relatively high values with the obtained falling between 5.11×10^{-3} – 2.02×10^{-2} SI (Table 2) and intensity 0.15–1.99 A/m. All these values are typical of mean magnetic susceptibility (K_m) governed by the ferromagnetic fraction^[3], and thus paramagnetic minerals can clearly be discounted because their mean susceptibilities are on the order of 5×10^{-4} SI^[13,14] which are about two orders of magnitude less than most susceptibilities of this study. Consistently high T_c from thermomagnetic analysis (Figure 2) indicates relatively uniform chemical composition of magnetic phases in the sills. Most specimens were characterized by high values (Königsberger ratio $Q' > 1$) (Figure 4(a)), indicating finer grains in single-domain (SD) or pseudo-single-domain (PSD) states most contribute to stable remanence; while some specimens from sites S3-6, 13 and 14 illustrate $Q' < 1$ (Figure 4(a)), consistent with partial contribution from larger PSD or multidomain (MD) magnetic grains.

Variations due to grain size and mineralogy can be inferred by means of hysteresis measurements. Two ratios (J_{rs}/J_s , the ratio of saturation remanence to saturation magnetization, H_{cr}/H_c , remanent coercive force to coercive force) are calculated as shown in Table 1 and representative hysteresis curves are revealed in Figure 4

(b), (c), (d), for samples from different sites obtained with a Molspin vibrating sample magnetometer. This instrument is sufficient to saturate TM and titanomaghemite grains but not fine-grained hematite with the maximum field of 1.14 T^[3]. Both ratios and H_c (coercive force) point toward PSD-like characteristics^[15] in most specimens. However, the interpretation of the domain state is somewhat ambiguous in that both types of igneous rocks possibly contain the mixtures of varying grain sizes and different magnetic minerals^[11,15], and a mixture of SD+MD grains cannot be ruled out, since Day’s limits for PSD data^[15] agree well with SD+MD properties according to revised limits recently proposed by Dunlop^[16,17]. As shown in Table 1, the ratio of J_{rs}/J_s and H_{cr}/H_c falls in the range 0.2–0.3 and 1.5–2.5, respectively, and H_c lying in 13.5–20 mT in most sills, 0.1–0.3 and 1.6–2.6 and 5.4–18.2 mT for the majority of basalts. Extremely finer subdivision of magnetic grains likely gives rise to the higher coercivities and J_{rs}/J_s ratio in the sills than in the basalts, agreeing with the mixture of smaller PSD or SD+MD magnetic domain state of the sills and slightly larger PSD states of the basalts. Nevertheless, a mixture of PSD and SD grains is possibly present in the sills^[18]. Two samples show the higher ratio of H_{cr}/H_c , possibly indicating the presence of superparamagnetic (SP) grains in the basalts^[15–17].

In summary, it appears that the sills show more homogeneous magnetic properties than the basalts and mainly contain smaller PSD or SD+MD magnetic minerals (TM and pure magnetite) carrying magnetic remanence, and ilmenite-lamellae corresponds to slow cooling rate. The basaltic flows more often have TM grains and magnetite in some case, fine skeleton grains suggesting the rapid cooling rate.

3 AMS of the sills and basalts

AMS is generally a complex phenomenon due to the mixed contribution of different magnetic minerals and domain states to the overall anisotropy of a sample. AMS measurements were carried out on 180 unheated samples with the KLY-2 kappa-bridge in the paleomagnetism laboratory at University of Bergen, and after progressive step heating to 600°C for 128 samples. The AMS parameters are defined using K_1 , K_2 and K_3 to denote maximum, intermediate and minimum susceptibility axes.

As revealed in Figure 5 (a) and Table 2, in the sills-magnetic susceptibility increased after heating above

Table 1 Hysteresis parameters of the sills and basalts.

Rock types	N	H_c (mT)	J_{rs}/J_s	H_{cr}/H_c
Sills	22	16.45±3.08	0.32±0.19	1.22±0.96
Basalt flows	17	11.81±6.37	0.21±0.11	2.02±1.93, 9.25, 13.87

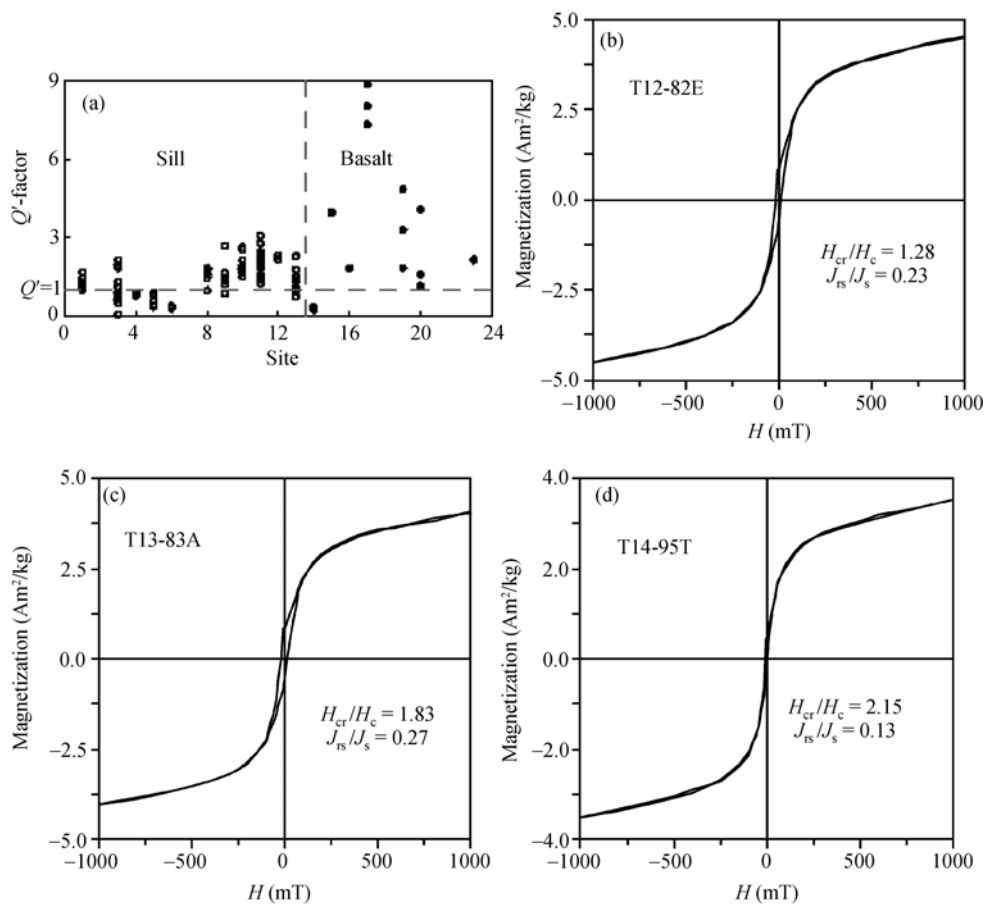


Figure 4 Q' -factor plot (a) illustrating the possible magnetic domain-type for sills and basalts; hysteresis curves for the sills (b) and (c), and for the basalts (d). The modified ratio $Q'=(10^7/4\pi)*(J_r/kH)$ SI, where H is the magnitude of the present geomagnetic field. $H_c = 15.04$ mT, 17.25 mT, 7.35 mT for T12-82E, T13-83A and T14-95 T, respectively.

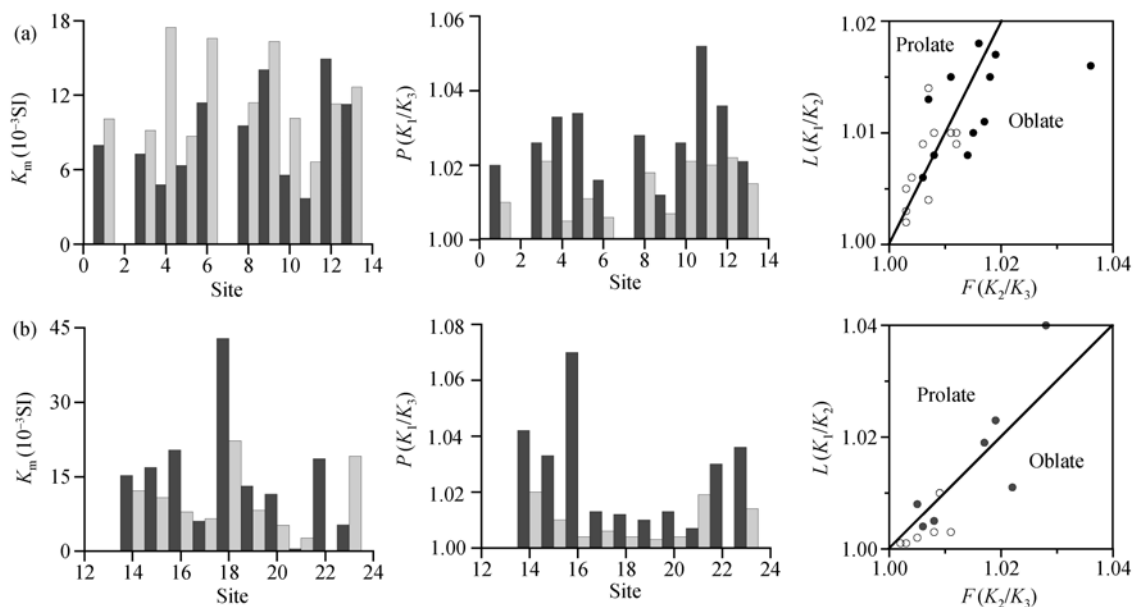


Figure 5 Profiles of mean magnetic susceptibility K_m , anisotropy degree (P), and Flinnplot for sills (a) and basalts (b) before (black) and after (grey columns and open circles) heating the selected samples. Foliation (F) vs. lineation (L) diagrams indicate the shape of the anisotropy of magnetic susceptibility ellipsoid.

Table 2 AMS parameters with standard deviations for the N specimens measured

		Unheated			
Rock types	N	$K_m(10^{-3} \text{ SI})$	P	L	F
Sills	106	8.806±5.617	1.022±0.012	1.010±0.006	1.011±0.006
Basalt flows	28	12.644±7.537	1.052±0.019	1.028±0.013	1.027±0.010
		Heated			
Rock types	N	$K_m(10^{-3} \text{ SI})$	P	L	F
Sills	63	11.859±5.423	1.009±0.006	1.004±0.003	1.002±0.003
Basalt flows	40	10.030±6.951	1.019±0.004	1.012±0.003	1.008±0.002

600°C mainly due to chemical conversion, growth of new oxides, or grain size variation^[3,4,19–21] corresponding to transformation SD-PSD-MD^[21]; the newly formed ferrimagnetic minerals such as magnetite minerals, converted from non- or less magnetic phases, develops within original crystals, giving rise to a strong increase in susceptibility^[3,4,19–21]. In contrast, K_m decreased in the basalts (Figure 5(b); Table 2), likely indicating the disappearance of ferrimagnetic minerals (such as oxidation of magnetite to hematite), converted to non- or less magnetic phases through alteration of magnetic minerals, transformation of magnetic phases or the producing of SD-PSD state upon heating up^[3,4,16,17,20]. The homogenization of the distribution of crystal defects and the inversion by filling up by new cations of the vacancy sites within the crystal lattice are responsible for significant K_m variation^[21]. P (K_1/K_3) was generally low (Figure 5(a), (b); Table 2), with most sill samples yielding average values 1.010–1.034 before heating and 1.003–1.015 after heating, the basalts, 1.033–1.071 and 1.015–1.023, which are the usual for igneous rocks with a primary magnetic fabric^[14,22,23]. Heating leads to a general decrease of P (Figure 5(a), (b); Table 2), may be due to the removal of secondary anisotropies related to tectonics^[24] and low temperature oxidation, implying a primary emplacement effect overlain by spurious secondary AMS components^[3]. In addition, alteration of magnetic minerals and formation of new magnetic phases further contribute to a lowering of anisotropy. Both values L (K_1/K_2) and F (K_2/K_3) show a decrease after heating (Table 2). In the sills and unheated basalts, the shape of the AMS ellipsoid has no significant tendency towards either an oblate or a prolate fabric (Figure 5(a), (b)), indicating that there is no predominance of magnetic foliation over magnetic lineation, similar to what Knight and Walker^[25] found in the Hawaiian basic dyke, but the heated basaltic sites are preferentially dominated by a consistent oblate pattern (Figures 5(b), 6). Nevertheless some show oblate ellipsoids, some

prolate ones and others triaxial ellipsoids (S11, unheated S17 and S19) in both the sill and unheated basaltic sites.

The distribution of AMS principal axes is presented in Figure 6. It appears that sites S1, S5, S10, S11 and S13 from sills underwent shallow-inclined K_1 axes move out of the plane of bedding and towards the bedding normal, K_2 and K_3 axes move toward the bedding plane, resulting in an improved definition of K_1 axes after heating to 600°C; accordingly, ellipsoid shapes also change (i.e. pre-heating shapes of S1 and S5 are predominantly prolate and S10, S11 and S13 reveal oblate ones, and after heating S10 and S13 demonstrate prolate ellipsoids and others are mixed by prolate and oblate) as shown in Figures 5(a), (b) and 6. K_1 and K_2 axes in S5 acquire a 90° move by exchanging position, and K_3 axes have not obvious change. A transition from PSD or larger grains to finer (SD) ones could cause the swap of K_1 and K_3 axes when grains are controlled by uniaxial shape anisotropy^[3,26]. This mechanism could explain both the change in ellipsoid shape and minimum axis orientation, and is consistent with the observation that the sills may contain PSD or SD+MD grains^[18]. Sites S17 and S19 from the basalts underwent significant axis shift, with K_1 and K_2 axes exchanging position; interestingly, K_3 axes relatively keep stable and post-heating fabrics become slightly worse defined. Site S16 with prolate ellipsoid shape acquired better defined fabrics and oblate feature during heating. Laboratory heating of Taimyr igneous rocks yields more information on changes in effective magnetic properties, and post-heating fabric is sometimes similar to the initial fabric such as S11, the inverse of the initial fabric^[3,5,19,26] or has differently oriented axes such as S5, S13, etc. Heat treatment can not only enhance pre-heating fabrics (S1) but also result in slightly worse defined post-heating fabrics (S17 and S19). Variations of susceptibility axes and ellipsoid shapes correspond to the ferrimagnetic minerals occurred or disappeared during the heat treatment^[19,21].

Inverse magnetic fabrics have been observed previ-

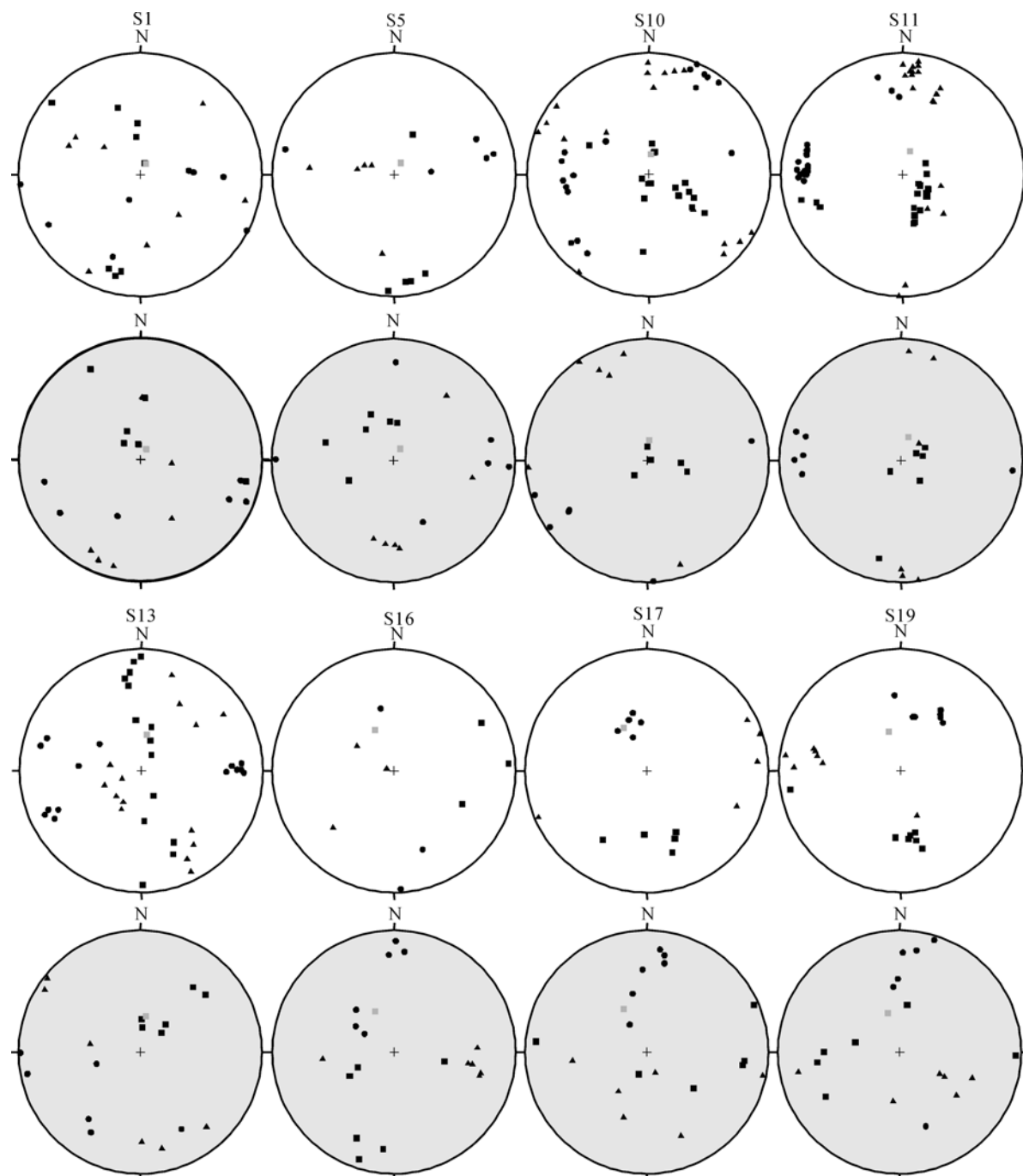


Figure 6 Stereoplots of the AMS axes before (open) and after (grey) heating at 600°C for sites S1, S5, S10, S11, S13, S16, S17 and S19. Low hemisphere. ■, K_1 ; ▲, K_2 ; ●, K_3 ; +, bedding pole.

ously and have been ascribed to either SD magnetite^[3,18,26,28], the paramagnetic mineral siderite or Fe-rich calcite^[26,27]. It is well known that SD magnetite has an inverse magnetic fabric^[26], with its K_1 axes normal to the basal plane (sites S10, S11, heated site S5, etc. in Figure 5), as opposite to the normal fabric in which K_3 axes should be perpendicular to the bedding and parallel to the bedding poles (unheated sites S17, 19 in Figure 6).

Partial contributions of SD and PSD or MD magnetite may yield intermediate fabrics, with K_2 axes normal to the bedding plane and K_1 and K_3 on the plane, or with no consistent orientation (unheated sites S1, S5, S13, etc. in Figure 5). In this case, magnetic mineralogy has confirmed the possibility of SD behavior which always leads to the axis inversion during AMS measurement^[3,18,26,29].

4 Discussion

The combined use of rock magnetic techniques leads us to suggest that the sills contain Ti-poor TM grains, and low to medium-Ti TM is the principal magnetic phase and hematite is a secondary for the basalts flows. Low-Ti TM has been reported from deep-buried oceanic lavas^[30] and from postulated shallow-water extrusives^[24,31]. The variation of magnetic properties across the Taimyr igneous rocks is not only due to grain-size variations, but also due to the concentration of magnetic minerals. Secondary, low-temperature alteration ranging from moderate (Figure 3(a)) to quite severe (Figure 3(b), (c)) has taken place in the sills. This would lead to a significant reduction in effective magnetic grain size in the sills, leaving magnetic grains closer to stable TM carriers of PSD and/or SD size. Smaller grain size as well as easier access of water to mix with minerals and oxygen due to cracks, contributes to the oxidation process^[3,19] of the rocks. Optical microscope observations suggest that some slight secondary magnetite, in correspondence to T_c close to 580°C, has formed in the sills prior to laboratory heating. Smaller grain sizes in the primary TM phase are therefore unlikely to be the sole cause of magnetic fabric. Grains of different sizes are possible to coexist in the same rock sample^[18]. Rock magnetic and the bulk magnetic property analysis clearly indicate that the sills contain SD or finer PSD magnetic grains^[18] even if the physical grain size observable under a microscope is larger in the sills than in the basaltic flows, while the effective magnetic grain size might be more towards coarser PSD in the basalts. The ferromagnetic contribution to AMS is dominant in the Permo-Triassic sills and basalts. Newly formed ferromagnetic grains during heating either simply replace pre-existing ones or correspond to exsolution from pre-existing minerals^[3,5,19,21,22]. A relative decrease of P in Taimyr igneous rocks on heating is in contrast with the results of Henry^[21] but consistent with that of Walderhaug^[3]. Strongly defined fabrics have been reported^[3,19,26,27], but heating has caused changes other than a simple modification or enhancement of the fabric^[21]. Laboratory heating does not simply enhance pre-heating fabric, and post-heating fabric is a composite one, resulting from the initial fabric and a new fabric related to the products of mineralogical changes^[21,32]. Since a rock is a multimineral system, changes in magnetic properties cannot be simply interpreted as the breakdown of a single min-

eral phase, but all mineral phases must be considered.

The interpretation of magnetic fabric is not always clear^[5]. Individual AMS components may relate to magma-flow directions, cooling stress, and tectonic stress associated with the magma emplacement^[3,29], rendering any predictions of “expected” initial AMS directions uncertain. Ellwood^[32] suggested that some secondary effects, where the K_3 is horizontally directed, maybe caused by thermally directed stress. Using computer modelling Dawson and Hargraves^[33] found that K_1 axes of a flowing magma point to the flow direction and K_3 are aligned perpendicular to the dyke wall, and that K_1 approximate the pole of a dyke wall when the magma is stationary. As a tabular intrusive structure parallel to any planes or layer in the country rock, a sill cannot agree with the flow direction sub-perpendicular to the bedding; however, the studied sill agrees with the second case where K_1 axes are the bedding normal. A large scatter in K_2 and K_3 directions is mainly considered to be poorly defined fabric due to low-magnetic foliation. Interpretation of the sill anisotropy in terms of the above model is therefore problematic, but a primary flow-controlled magnetic fabric remains a possibility; nevertheless, further work to determine the domain state of the magnetic minerals will be needed to better study the magma emplacement.

5 Conclusion

The mean magnetic susceptibility (K_m) for all igneous rocks is usually high ($>3.7 \times 10^{-3}$ SI for the sills and $>5.3 \times 10^{-3}$ SI for the basaltic flows; Table 2, Figure 5). Variations in magnetic properties across these rocks are caused by varying TM concentration as well as grain size. Grains of smaller sizes carry the most stable remanent magnetization.

AMS is dominantly carried by ferromagnetic minerals. Fine (smaller PSD and SD) as well as coarse (larger PSD- or MD-like) Ti-poor TM grains up to pure magnetite are main magnetic minerals in the sills, whereas for the basalts, the magnetic minerals may be more toward low to medium-Ti TM grains in larger PSD or MD size. The inverse fabric was recognized (Figure 6) in the studied sill, possibly contributed by SD magnetic minerals.

Heat treatment produces AMS changes, which does not always correspond to simple enhancement of the magnetic fabric for all samples, and in some cases the opposite is true, because heating leads to transformation

of magnetic minerals, formation of new magnetic minerals and new grain sizes. Post-heating fabric possibly results from the pre-heating fabric and a new fabric related to new minerals produced during heating. Corresponding alteration of magnetic parameters occurred during heating. The quality of AMS data at each site have to be observed on heated samples to determine whether there is obvious benefit achieved by thermal

treatment.

We gratefully acknowledge the economic support from Norwegian Research Council as a grant to HJW, Norwegian State Education Loan Fund, and thoroughly logistic support of SWEDARP and EUROPROBE. We appreciate all personnel at the Paleomagnetism Laboratory (University of Bergen) for getting used with the equipments. Shuwei Zhang is grateful for suggestions and helpful discussions by Dr. Shihong Zhang, Dr. Qingsong Liu, Dr. Yongjia Yu and Dr. Yigui Han. Thorough reviews by two anonymous referees substantially improved the final version of the paper.

- 1 Petersen N. Notes on the variation of magnetization within basalt lava flows and dikes. *Pageoph*, 1976, 114: 177–193[[doi](#)]
- 2 Ellwood B B, Balsam W, Burkart B, et al. Anomalous magnetic properties in rocks containing the mineral siderite: Paleomagnetic implications. *J Geophys Res*, 1986, 91: 12779–12790
- 3 Walderhaug H J. Rock magnetic and magnetic fabric variations across three thin alkaline dikes from Suunhord-land, Western Norway; influence of initial mineralogy and secondary chemical alterations. *Geophys J Int*, 1993, 115: 97–108[[doi](#)]
- 4 Liu Q S, Banerjee K S, Jackson J M, et al. New insights into partial oxidation model of magnetites and thermal alteration of magnetic mineralogy of the Chinese loess in air. *Geophys J Int*, 2004, 158: 506–514[[doi](#)]
- 5 Tarling D H, Hrouda F. *The Magnetic Anisotropy of Rocks*. London: Chapman & Hall, 1993
- 6 Bezzubtsev V V, Malitch N S, Markov F G, et al. Geological map of mountainous Taimyr, 1:500 000. Ministry of Geology of the USSR. Ministry of Geology of the Russian Federation (RFSFR), Krasnoyarskgeologia, Krasnoyarsk (in Russian), 1983
- 7 Torsvik T H, Andersen T B. The Taimyr fold belt, Arctic Siberia: timing of pre-fold remagnetisation and regional tectonics. *Tectonophysics*, 2002, 352: 335–348[[doi](#)]
- 8 Egorov A Yu, Kulikova L I. Stratigraphic position of the Early Triassic traps on the Taimyr Peninsula. *Trudy IgiG SO AN SSSR (in Russian)*, 1989, 732: 91–101
- 9 Mogucheva N K, Betekhtina O A. Urgent problems of the stratigraphy of the continental Siberian Triassic. *Geol Geofiz*, 1998, 39: 293–302
- 10 Inger S, Scott R A, Golionko B G. Tectonic evolution of the Taimyr Peninsula, northern Russia: implications for Arctic continental assembly. *J Geol Soc*, 1999, 156: 1069–1072[[doi](#)]
- 11 Walderhaug H J, Eide E A, Scott R A, et al. Palaeomagnetism and $^{40}\text{Ar}/^{39}\text{Ar}$ geochronology from the South Taimyr igneous complex, Arctic Russia: a Middle-Late Triassic magmatic pulse after Siberian flood-basalt volcanism. *Geophys J Int*, 2005, 163: 1–17
- 12 Zhang S H, Li P J, Wang L B. Study of Jisu basalt from Jilin Province and magnetic fabrics of its country rocks. *Chin Acta Geophys Sin (in Chinese)*, 1994, 37(Suppl 1): 316–323
- 13 Wagner J J, Hedley F G, Steen D, et al. Magnetic anisotropy and fabric of some progressively deformed ophiolitic gabbros. *J Geophys Res*, 1981, 86: 307–315
- 14 Hrouda F. Magnetic anisotropy of rocks and its application in geology and geophysics. *Surv Geophys*, 1982, 5: 37–82[[doi](#)]
- 15 Day R, Fuller M, Schmidt V A. Hysteresis properties of titanomagnetites: grain size and compositional dependence. *Phys Earth Planet Inter*, 1977, 13: 260–267[[doi](#)]
- 16 Dunlop D J. Theory and application of the Day plot (M_{rs}/M_s versus H_{cr}/H_c): 1. Theoretical curves and tests using titanomagnetite data. *J Geophys Res*, 2002, 107: 10.1029/2001 JB000487
- 17 Dunlop D J. Theory and application of the Day plot (M_{rs}/M_s versus H_{cr}/H_c) 2. Application to data for rocks, sediments, and soils. *J Geophys Res*, 2002, 107, doi: 10.1029/2001 JB000487
- 18 Zhang S W, Walderhaug H J, Yang Y J. Magnetic fabric and its significance in igneous rocks from Taimyr fold-belt, Arctic Siberia. *Geophys J Int* (submitted)
- 19 Pan Y X, Zhu R X, Banerjee S K, et al. Rock magnetic properties related to thermal treatment of siderite: Behavior and interpretation. *J Geophys Res*, 2000, 105: 783–794[[doi](#)]
- 20 Hirt A M, Gerhring A U. Thermal alteration of the magnetic mineralogy in ferruginous rocks. *J Geophys Res*, 1991, 96: 9947–9953
- 21 Henry B, Jordanova D, Jordanova N, et al. Anisotropy of magnetic susceptibility of heated rocks. *Tectonophysics*, 2003, 366: 241–258[[doi](#)]
- 22 Staudigel H G, Gee G, Tauxe L, et al. Shallow intrusive direction of sheeted dykes in the Troodos ophiolite: anisotropy of magnetic susceptibility and structural data. *Geology*, 1992, 20: 841–844[[doi](#)]
- 23 Callot J P, Geoffroy L, Aubourg C, et al. Magma flow directions of shallow dykes from the East Greenland volcanic margin inferred from magnetic fabric studies. *Tectonophysics*, 2001, 335: 313–329[[doi](#)]
- 24 Park J K, Tanczyk E, Debarats A. Magnetic fabric and its significance in the 1400 Ma Mealy diabase dykes of Labrador, Canada. *J Geophys Res*, 1988, 93: 13689–13704
- 25 Knight M D, Walker G P L. Magma flow directions in flows of the Koolau Complex, Oahu, determined from magnetic fabric studies. *J Geophys Res*, 1988, 93: 4308–4319
- 26 Potter D K, Stephenson A. Single-domain particles in rocks and magnetic fabric analysis. *Geophys Res Lett*, 1988, 15: 1097–1100
- 27 Rochette M J, Aubourg C. Rock magnetism and the interpretation of anisotropy of magnetic susceptibility. *Rev Geophys*, 1992, 30(3): 209–226
- 28 Rochette P. Inverse magnetic fabric in carbonate-bearing rocks. *Earth Planet Sci Lett*, 1988, 90: 229–237[[doi](#)]
- 29 Dragoni M, Lanza R, Tallarico A. Magnetic anisotropy produced by magma flow: theoretical model and experimental data from Ferrar dolerite sills (Antarctica). *Geophys J Int*, 1997, 128: 230–240[[doi](#)]
- 30 Smith G M, Banerjee S K. Magnetic properties of basalts from Deep Sea Drilling Project Leg 83: the origin of remanence and its relation to tectonic and chemical evolution. *Init Rep DSDP*, 1985, 83(b): 347–357
- 31 Cockerham R S, Hall J M. Magnetic properties and paleomagnetism of some Leg 33 basalts and sediments and their tectonic implications. *J Geophys Res*, 1976, 81: 4207–4222
- 32 Ellwood B B. Anisotropy and magnetic susceptibility variations in Icelandic columnar basalts. *Earth Planet Sci Lett*, 1979, 42: 209–212[[doi](#)]
- 33 Dawson E M, Hargraves R B. Anisotropy of magnetic susceptibility as an indicator of magma flow directions in diabase dykes (abstract). *Eos Trans AGU*, 1985, 66: 251